Analysis of Ar line spectra from indirectly-driven implosion experiments on SGII facility*

Pu Yu-Dong(蒲昱东)†, Zhang Ji-Yan(张继彦), Yang Jia-Min(杨家敏), Huang Tian-Xuan(黄天晅), and Ding Yong-Kun(丁永坤)

Research Center of Laser Fusion, China Academy of Engineering Physics, Mianyang 621900, *China*

(Received 1 June 2010; revised manuscript received 21 July 2010)

This paper reports on the indirectly-driven implosion experiments on SGII laser facility in which Ar emission spectrum from Ar-doped D-filled plastic capsule is recorded with the crystal spectrometer. Spectral features of Ar Heβ line and its associated satellites are analysed to extract the electron temperature and density of the implosion core. Non local thermal equilibrium (NLTE) collisional-radiative atomic kinetics and Strark broadening line shape are included in the present calculation. By comparing the calculated spectrum with the measured one, the core electron temperature and density are inferred to be 700 eV and 2.5×10^{23} cm^{-3} respectively. With these inferred values of electron temperature and density, neutron yield can be estimated to agree with the measured value in magnitude despite of the very simple model used for the estimation.

Keywords: inertial confinement fusion, x-ray diagnostics

PACS: 52.27.–z, 52.70.–m **DOI:** 10.1088/1674-1056/20/1/015202

1. Introduction

In recent years, much works have been devoted to the researches of inertial confinement fusion.[1] Under the scheme of central ignition, a hot spot is formed by symmetrical ablative compression of the gas-filled capsule. Understanding the conditions in the hot spot is essential for us to understand the implosion physics as well as the numerical simulation results.[2] Usually there are two effective ways to obtain information on the implosion core, one is the measurement of nuclear reaction productions, and the other is spectroscopic diagnostics. In neutron diagnostics, secondary neutrons could be used for the determination of the imploded fuel areal density,[3] and the neutron energy spectrum width could be used to infer the ion temperature in the hot spot.[4] But in current experiments, relatively low neutron yields limit the applications of these methods. Instead, spectroscopic diagnostics is used as the other way to study the hot spot conditions. This method consists of adding small concentrations of mid-Z dopant into the fuel, and measuring the K-shell emission at the collapse of the implosion. In the case of our experiments, 1% Ar of atomic number is seeded in the capsule and time-integrated spectrum is recorded with the crystal spectrometer. As mentioned by Hammel,[5] the intensity ratio of the Heβ line to its associated satellites is sensitive to the temperature, and the shape of Heβ line is sensitive to the density. So we have analysed the spectral features of Heβ line and its associated satellites, namely Heβ complex, to extract electron temperature and density in the hot spot. Comparing with the work in Refs. [6] and [7], we have got rid of the assumptions of local thermal equilibrium (LTE), which is unlikely the real situation in the hot spot, by using a non-LTE collisional radiative model to calculate the level populations. We also explicitly include the effects of electron collisional broadening in our calculation instead of an approximated way to improve the accuracy in the central portions of the line profile.

2. Experimental details

The indirectly-driven implosion experiments discussed here were performed on SGII laser facility. As shown in Fig. 1, the incident laser energy with total energy of 2 kJ is directed into a gold cylindrical hohlraum and converted to x-rays which are used to drive a capsule with a plastic ablator. The hohlraum is 1200 μm in length, 800 μm in radius, and with a

*Project supported by the Science and Technology Foundation of State Key Laboratory of Plasma Physics (Grant No. 9140C6805100C68).

†Corresponding author. E-mail: pyd02@mails.tsinghua.edu.cn

© 2011 Chinese Physical Society and IOP Publishing Ltd

diagnostic hole on the side. A slit of 13 μm width is placed in the front of the diagnositc hole to provide a spatial resolution of 14.5 μm in the observed energy region. The capsule has an initial diameter of 220 μm, a plastic wall of 15 μm, and is filled with 1.5 mg/cm^3 of DD and 1% Ar at atomic level. Ar K-shell emissions are dispersed with polythylene terephthalate (PET) crystal onto TJ-III films with spectral resolving power $\lambda/\Delta\lambda$ of $\sim$500. We digitized the film with densitometer and corrected the sensitivity of the film. Thus, from the obtained time-integrated and space-resolved spectrum, we can see that the spatial size of the emission core is approximately 20 μm in diameter which is comparable to the spatial resolution. Since the detailed structure of the implosion core cannot be well resolved, only the space-integrated spectrum is involved in the following disscusion.

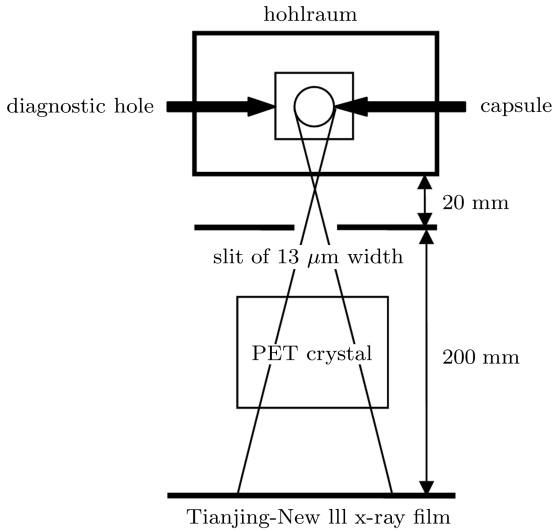


Fig. 1. Experimental configuration. Eight laser beams, 4 per laser entrance hole (LEH), are directed into the gold cylindrical hahlraum with total energy of 2 kJ.

3. Data analysis

Figure 2 shows a typical space–time integrated spectrum recorded in our experiments. The Heα, Heβ, Heγ, and Lyα line are identified. The peak on the blue side of Heβ is unlikely emitted by Ar ions, may come from the Au plasma near the diagnostic hole. Since the intensity of Lyα is relatively small, it is reasonable to think of a low temperature in the implosion core. This deduction can be further proved by the evident appearance of satellite features, and is consistent with the calculated results. In order to obtain a further insight into the measured spectrum, we use a model including nonequilibrium collisional-radiative atomic kinetics and Strark broadening line shape to analyse the Heβ complex which is estimated to be optically thin. Detailed model description will be given below.

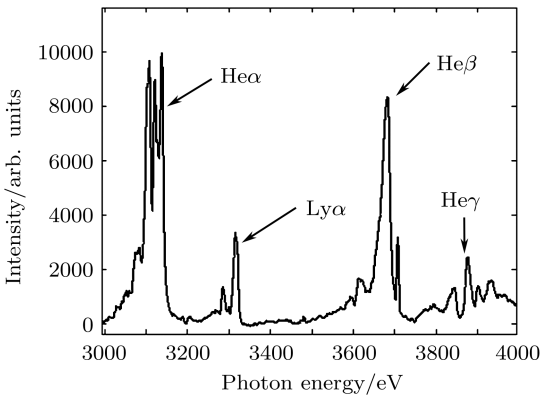


Fig. 2. Typical measured spectrum. The spectrum is recorded with spectral resolving power of $\sim$500.

The NLTE model[8] includes ionization stages from fully-tripped ions to N-like ions. Only ground states are included for ionization stages beyond B-like ions, while for other ionization stages singly excited states are included up to $n = 5$. Since high order satellites have significant effects on the line shape of red wing, doubly excited states of $2lnl'$ ($n = 2$, 3, 4) and $3lnl'$ ($n = 3$, 4) are considered for He- and Li-like ions. All the atomic parameters, like energy levels and cross sections of various transition processes, are calculated by Flexible Atom Code (FAC)[9] in which atomic structure is calculated by Dirac–Fork–Slater methods with configuration mixing. Level populations are then obtained by solving the rate equation in steady state approximation. The line intensity ratios of the satellites to the Heβ line are shown in Fig. 3 as a function of electron temperature for electron density equal to 2.5×10^{23} cm^{-3}.

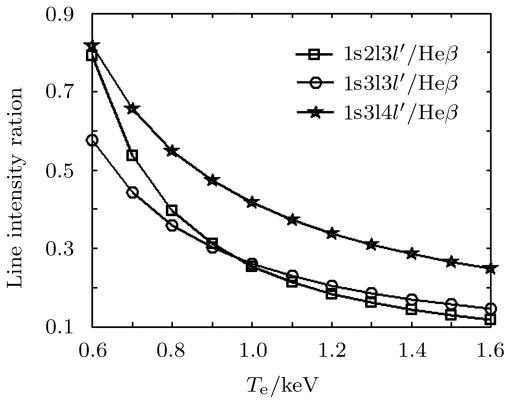


Fig. 3. Line intensity ratios of satellites to Heβ line as a function of electron temperature for electron density of 2.5×10^{23} cm^{-3}.

Stark broadening shapes are calculated for Heβ resonant line, while profiles of its satellites are approximated by Lorentz profile with the same full width at half maximum (FWHM) as the resonance line. The spectral line broadening calculation is based on a relaxation theory developed by Smith.[10] The primary broadening mechanism considered here is the interaction between a radiating atom and the electric field produced by surrounding ions and electrons. Since the perturbing ions can be regarded as stationary during the emission process, the effects of perturbing ions on the radiating atom can be approximated by ion microfield which is calculated by Hooper's[11,12] method. Electron collisional broadening is treated without impact approximation,[13] and can be regarded as a result of the quadratic Stark interaction between the electron microfield and the radiating atom. Electron correlations,[14] and distortions of plane wavefunctions of free electrons[15] by charged radiating ions is also considered. Atomic parameters needed in the line profile calculations, like transition energy, spontaneous emission rate and radial wavefunctions, are also calculated by FAC. The transition matrix elements of multi-electron ions are calculated via the Wigner–Eckart theorem[16] using wavefunctions produced by FAC. Figure 4 shows the areal normalized profiles of Heβ line shape with different electron densities. These profiles have convolved with instrument broadening about ∼3 eV in FWHM and are insensitive to variations of electron temperature.

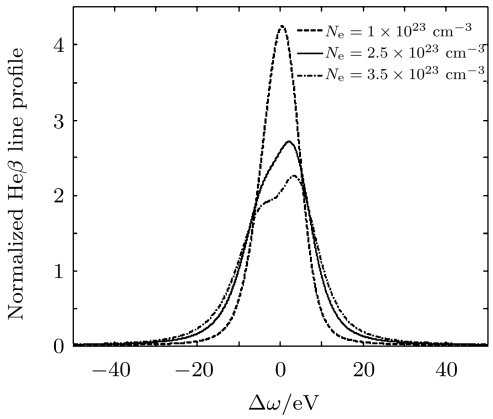


Fig. 4. The areal normalized profiles of Heβ line shape with different electron densities. These profiles have convolved with instrument broadening about ∼3 eV in FWHM and are insensitive to variations of electron temperature.

Before comparing the calculated spectrum of Heβ complex with the measured one, self-absorption effects is considered by radiation transfer in uniform plasma with plane geometry.

$$I(h\nu) = S(h\nu)(1 - \mathrm{e}^{-\tau(h\nu)}),$$

where $S(h\nu) = j(h\nu)/\kappa(h\nu)$ is the source function. $j(h\nu)$ and $\kappa(h\nu)$are the emission coefficient and absorption coefficient respectively. The absorption length used for the calculation of $\tau(h\nu)$ is approximated to be the average chord length of the hot spot whose diameter can be estimated by assuming spherical implosion and mass conservation.

In order to find the conditions on which the measured spectral features of Heβ complex can be best fitted, we performed calculations on N_e–T_e grids using NLTE populations and Stark broadening line shape. The best fit is found with electron temperature and density equal to 700 eV and 2.5×10^{23} cm^{-3} respectively, and is shown in Fig. 5.

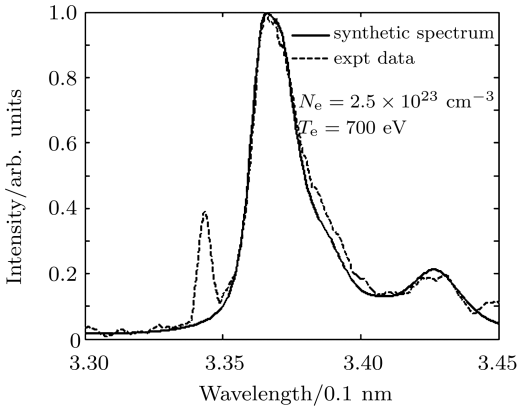


Fig. 5. Synthetic spectrum calculated with $N_e = 2.5 \times 10^{23}$ cm^{-3}, $T_e = 700$ eV. The measured spectrum is best fitted.

We also show in Fig. 6 individual contributions of each line transition to the composite spectra. High order satellites contribute significantly to the Heβ red wings, and is necessarily considered to properly describe the measured satellite features.[17] We believe that the accuracy of the inferred electron temperature is about 30% according to the comparison between our calculated line ratios with that obtained by Keane,[18] while the accuracy of the inferred electron density is about 20% according to Regan's comments[19] on this diagnostic method and comparison between our calculated Heβ profile with Mancini's one.[20] All the conclusions on the accuracy mentioned above are proper when only the method uncertainties for level population and line profile calculations are considered. Experimental uncertainties, like film responses and uniform plasma assumptions, are not addressed in the present work.

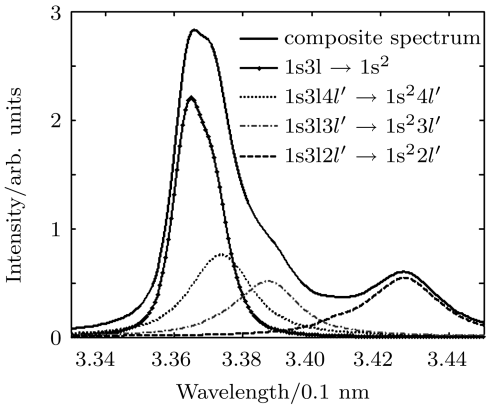


Fig. 6. Individual contributions of each line transition to the composite spectra on the condition of best fit. High order satellites contribute significantly to the Heβ red wings.

As a rough check of the inferred electron temperature and density in the hot spot, we use a simple model to estimate the neutron yield and compare it with the measured one. The neutron yield can be estimate as follows:

$$Y_n = \frac{1}{2} N_{\rm e}^2 \langle \sigma V(T_{\rm e}) \rangle \, \tau \, \Delta V_h,$$

$$\Delta V_{\rm h} = \frac{4}{3} R_{\rm i}^3 \rho_{\rm i} N_{\rm A}/(N_{\rm e} M) = 1.26 \times 10^{24} \frac{\rho_{\rm i} R_{\rm i}^3}{N_{\rm e}},$$

where $\rho_{\rm i}({\rm g/cm^3})$ and $R_{\rm i}({\rm cm})$ are the initial filled gas density and the initial radius of the capsule respectively. Since the measured neutron yield is relatively small, burning efficiency of D ions must be very small which makes the assumption of constant ion density to be justified. The ion temperature is taken as the electron temperature, and the ion density is assumed to be uniform in a spherical hot spot. The burning time (τ) is estimated to be 100 ps,[21] which is the confinement time of the capsule. The averaged cross section is taken from Ref. [21]. At last, we notice that the estimated neutron yield is 2.25×10^5 which agrees the measured one 1.8×10^5 in magnitude despite of the very simple model used for the estimation. We should notice that the ion temperature in the hot spot is always higher than the electron temperature according to simulation results.[21] Since the cross sections are sensitive to the ion temperature, so the estimated neutron yield should be even larger when the ion temperature instead of electron temperature is used for the estimation. We also neglect the temperature and density gradients as well as their transient properties in our estimation. These effects will be considered in detail in further works.

4. Summary

By analysing the Heβ spectral features, we inferred electron temperature and density in the implosion core. In modeling the measured spectrum, nonequilibrium collisional-radiative atomic kinetics and Stark broadening line shape are included and fairly good agreement is achieved. But currently, spatial gradients as well as time evolutions of the hot spot are not modeled yet. The difference between time-space averaged calculations with the time-space resolved ones will be investigated in future work, and comparisons with results from radiation hydrodynamic simulations will be made. Besides, we will also devote to the satellite profile calculation and model the continuum spectrum.

References

[1] John D, Lindl, Peter Amendt and Richard L. Berger 2004 *Phys. Plasma* **11** 339
[2] Woolsey N C 1997 *Phys. Rev.* E **56** 2314
[3] Cable M D and Hatchett S P 1987 *J. Appl. Phys.* **62** 2233
[4] Chen J B, Zheng Z J and Peng H S 2001 *Rev. Sci. Instru.* **72** 3534
[5] Hammel B A 1993 *Phys. Rev. Lett.* **70** 1263
[6] Duan Bin 2007 *J. At. Mol. Phys.* 1000-0364(2007)supplement-001-04 (in Chinese)
[7] Duan B, Li M Y, Fang Q Y and Zhang J Y 2005 *High Power Laser and Particle Beams* **17** 55 (in Chinese)
[8] Pu Y D, Huang T X and Miao W Y 2010 *High Power Laser and Particle Beams* **22** (in Chinese)
[9] Gu M F 2003 *ApJ* **582** 1241
[10] Smith 1967 *Phys. Rev.* **157** 126
[11] Hooper 1966 *Phys. Rev.* **149** 77
[12] John T O'Brien 1972 *Phys. Rev.* A **5** 867
[13] Kolb A C 1958 *Phys. Rev.* **111** 514
[14] Smith 1968 *Phys. Rev.* **166** 102
[15] John T O'Brien 1974 *J. Quant. Spectrosc. Radiat. Transfer* **14** 479
[16] Cowan 1981 *The Theory of Atomic Structure and Spectra* (California: University of California Press)
[17] Golovkin I E 2000 *Journal Quant. Spect. Radiat. Transfer* **65** 273
[18] Keane C J 1993 *Phys. Fluids* B **3** 3328
[19] Regan S P 2002 *Phys. of Plasmas* **9** 1357
[20] Mancini 1991 *Computer Physics Communications* **63** 314
[21] Stefano Atzeni 2004 *Inertial Fusion Beam Plasma Interaction, Hydrodynamics, Dense Plasma Physics* (New York: Oxford University Press)